Tricarbonyl(carbaborane) Complexes of the Group 6 Metals as Reagents for preparing Heteronuclear Dimetal Compounds involving Platinum†

Stephen J. Dossett, Donald F. Mullica, Eric L. Sappenfield, F. Gordon A. Stone* and Michael J. Went
Department of Chemistry, Baylor University, Waco, TX 76798-7348, USA

The reagents $Tl_2[M(CO)_3(\eta^5\text{-}C_2B_9H_9Me_2)]$ (M = Cr, Mo or W), generated *in situ* from $Tl[TlC_2B_9H_9Me_2]$ and $[M(CO)_3(NCMe)_3]$, react in thf (tetrahydrofuran) with the compounds $[PtCl_2L_2]$ (L = PPh_3 or PEt_3) to give the dimetal complexes $[MPt(CO)_3L_2(\eta^5\text{-}C_2B_9H_9Me_2)]$. NMR studies revealed that the tungsten–platinum species were produced as a mixture of two isomers of formulation $[WPt(CO)_3L_2(\eta^5\text{-}C_2B_9H_9Me_2)]$ and $[WPt(\mu\text{-}H)(\mu\text{-}\sigma:\eta^5\text{-}C_2B_9H_8Me_2)(CO)_3L_2]$. The complexes $[MPt(CO)_3L_2(\eta^6\text{-}C_2B_{10}H_{10}Me_2)]$ have been prepared from reactions between $[PtCl_2L_2]$ and $Na_2[M(CO)_3(\eta^6\text{-}C_2B_{10}H_{10}Me_2)]$ (M = Mo or W), with the latter generated *in situ* from $Na_2[C_2B_{10}H_{10}Me_2]$ and $[M(CO)_3(NCMe)_3]$. Similar reactions using $[PtCl_2(cod)]$ (cod = cycloocta-1,5-diene), followed by addition of PPh_3 to the reaction mixture, afforded the salts $[PtH(PPh_3)_3][MPt(\mu\text{-}\sigma:\eta^6\text{-}C_2B_{10}H_9Me_2)(CO)_4(PPh_3)]$. Protonation ($HBF_4\cdot Et_2O$) of the latter yields the complexes $[MPt(CO)_4(PPh_3)(\eta^6\text{-}C_2B_{10}H_{10}Me_2)]$. An X-ray crystallographic study of the molybdenum–platinum compound revealed that the molecule contained a Mo–Pt bond [2.814(1) Å] spanned by the *nido*-$C_2B_{10}H_{10}Me_2$ cage such that the latter is η^6-co-ordinated to the molybdenum and linked to the platinum *via* a three-centre two-electron B–H→Pt bond. This bond involves the hydrogen atom attached to the boron atom which is β to the carbons in the CBC*B*B face of the cage ligating the molybdenum atom. The NMR data (^1H, $^{13}C\text{-}\{^1H\}$, $^{31}P\text{-}\{^1H\}$ and $^{11}B\text{-}\{^1H\}$) for the new compounds are discussed in relation to the structures proposed.

Salts of the anionic complexes $[M(\equiv CR)(CO)_2(\eta^5\text{-}C_2B_9H_9R'_2)]^-$ (M = W or Mo; R = alkyl, aryl or alkynyl; R′ = Me or H) are versatile reagents for preparing polynuclear metal complexes.[1] Reactions with platinum compounds, in particular, afford a variety of structurally interesting products.[2] In acetone, the salts $[N(PPh_3)_2][W(\equiv CC_6H_4Me\text{-}4)(CO)_2(\eta^5\text{-}C_2B_9H_9Me_2)]$ and $[PtH(Me_2CO)(PEt_3)_2][BF_4]$ yield $[WPt(CO)_2(PEt_3)_2\{\eta^6\text{-}C_2B_9H_8(CH_2C_6H_4Me\text{-}4)Me_2\}]$ **1a**, a complex in which the tungsten atom is a vertex in an unusual WC_2B_9 *hypercloso* framework.[2a] Treatment of **1a** with CO, however, gives $[WPt(\mu\text{-}H)\{\mu\text{-}\sigma:\eta^5\text{-}C_2B_9H_7(CH_2C_6H_4Me\text{-}4)Me_2\}(CO)_3(PEt_3)_2]$ **2a**, in which the structure of the WC_2B_9 cage has reverted to a *closo*-icosahedral framework, but one with an exopolyhedral B–Pt σ bond. The corresponding reaction between $[NEt_4][Mo(\equiv CC_6H_4Me\text{-}4)(CO)_2(\eta^5\text{-}C_2B_9H_9Me_2)]$ and the platinum reagent follows a similar pathway, but unlike **1a**, compound **1b** has only a transient existence, decomposing to complex **2b** at ambient temperatures.[2b]

In contrast with these results, the reaction between $[PtH(Me_2CO)(PEt_3)_2][BF_4]$ and $[NEt_4][W(\equiv CC_6H_3Me_2\text{-}2,6)(CO)_2(\eta^5\text{-}C_2B_9H_9Me_2)]$ initially yields $[WPtH(\mu\text{-}CC_6H_3Me_2\text{-}2,6)(CO)_2(PEt_3)(\eta^5\text{-}C_2B_9H_9Me_2)]$ **3**, which subsequently releases hydrogen affording $[WPt(\mu\text{-}CC_6H_3Me_2\text{-}2,6)(\mu\text{-}\sigma:\eta^5\text{-}C_2B_9H_8Me_2)(CO)_2(PEt_3)]$ **4**.[2c] The latter, like **2a** and **2b**, contains an exopolyhedral B–Pt bond, a type of linkage also found in the dimetal compounds $[MPt(\mu\text{-}CC_6H_4Me\text{-}4)(\mu\text{-}\sigma:\eta^5\text{-}C_2B_9H_8Me_2)(CO)_2(PMe_2Ph)_2]$ (M = W **5a** or Mo **5b**), obtained from the reactions between $[NEt_4][M(\equiv CC_6H_4Me\text{-}4)(CO)_2(\eta^5\text{-}C_2B_9H_9Me_2)]$ and $[PtCl(Me)(PMe_2Ph)_2]$ in the presence of $TlBF_4$.[2b,d] These syntheses are believed to involve release of methane. Moreover, the synthesis of **5a** is accompanied by that of an isomer (not shown) with the B–Pt linkage employing a boron atom α rather than β to the carbons in the C_2B_3 ring ligating the tungsten, while in the preparation of **5b** a further product is a molybdenum–platinum complex having one PMe_2Ph ligand replaced by a CO molecule.

The non-spectator role adopted by the carbaborane ligand in these dimetal compounds, all of which were derived from the anionic complexes $[M(\equiv CR)(CO)_2(\eta^5\text{-}C_2B_9H_9Me_2)]^-$, prompted consideration of other tungsten– and molybdenum–carbaborane reagents which might be used as precursors in related syntheses. In this paper we describe the preparation and characterisation of new tungsten– and molybdenum–platinum compounds employing salts of the anionic complexes $[M(CO)_3(\eta^5\text{-}C_2B_9H_9Me_2)]^{2-}$ and $[M(CO)_3(\eta^6\text{-}C_2B_{10}H_{10}Me_2)]^{2-}$ (M = Mo or W). Although the anionic molybdenum and tungsten species $[M(CO)_3(\eta^5\text{-}C_2B_9H_9Me_2)]^{2-}$ have been known for many years,[3a] until recently there have been few reports of their use in preparing mixed-metal complexes.[3b,c] This is surprising since these anions are mapped isolobally with the cyclopentadienyl species $[M(CO)_3(\eta^5\text{-}C_5H_5)]^-$, and a very extensive chemistry is associated with employment of salts of the latter in the syntheses of compounds with bonds between the Group 6 elements and other metals. Salts of the species $[M(CO)_3(\eta^6\text{-}C_2B_{10}H_{10}Me_2)]^{2-}$ have not been previously studied.

Results and Discussion

Treatment of a thf (tetrahydrofuran) suspension of $Tl[TlC_2B_9H_9Me_2]$[3b,4] with $[M(CO)_3(NCMe)_3]$ (M = Cr, Mo or W)

---

† In this paper metal atoms form with $[nido\text{-}7,8\text{-}C_2B_9H_9Me_2]^{2-}$ or $[nido\text{-}7,9\text{-}C_2B_{10}H_{10}Me_2]^{2-}$ dianions *closo*-1,2-dicarba-3-metalladodecaborane or *closo*-1,6-dicarba-4-metallatridecaborane structures, respectively. However, in the formulae the carbaborane groups are designated as $\eta^5\text{-}C_2B_9H_9Me_2$ or $\eta^6\text{-}C_2B_{10}H_{10}Me_2$ ligands in order to emphasise their penta-and hexa-hapto properties in which they formally act as four-electron donors.

Supplementary data available: see Instructions for Authors, *J. Chem. Soc., Dalton Trans.*, 1993, Issue 1, pp. xxiii–xxviii.

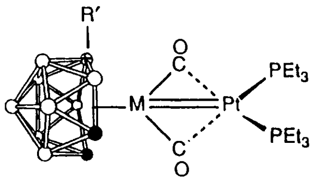

	M	R′
1a	W	$CH_2C_6H_4Me$-4
1b	Mo	$CH_2C_6H_4Me$-4
1c	W	CH_2Me
1d	W	H

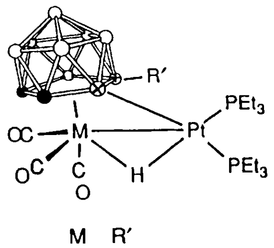

	M	R′
2a	W	$CH_2C_6H_4Me$-4
2b	Mo	$CH_2C_6H_4Me$-4
2c	W	CH_2Me
2d	W	H

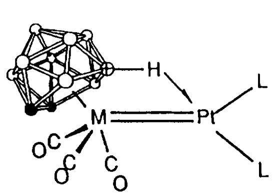

	M	L
6a	Cr	PPh_3
6b	Mo	PPh_3
6c	W	PPh_3
6d	Mo	PEt_3
6e	W	PEt_3

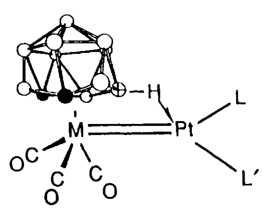

	M	L	L′
7a	Mo	PPh_3	PPh_3
7b	W	PPh_3	PPh_3
7c	Mo	PEt_3	PEt_3
7d	W	PEt_3	PEt_3
7e	Mo	PPh_3	CO
7f	W	PPh_3	CO

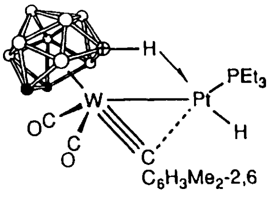

3

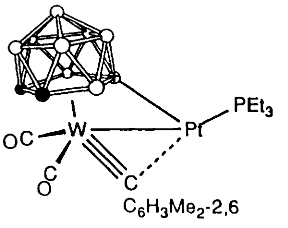

4

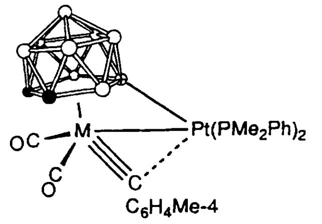

	M
5a	W
5b	Mo

● CMe ○ BH ⊕ B

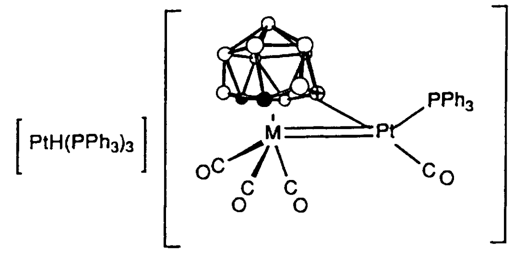

	M
8a	Mo
8b	W

● CMe ○ BH ⊕ B

followed by addition of $[PtCl_2(PR_3)_2]$ (R = Ph or Et) affords the bimetal compounds $[MPt(CO)_3(PR_3)_2(\eta^5-C_2B_9H_9Me_2)]$ **6**. Data characterising these new compounds are given in Tables 1–3. All the products display bands in their IR spectra in the range 1869–1858 cm^{-1}, and as discussed below this may indicate that in solution one of the CO ligands semi-bridges the metal–metal bond. With the exception of the chromium–platinum species **6a**, the complexes are reasonably stable in air or in solutions of organic solvents.

The NMR data for all the complexes were very informative. Those for the tungsten compounds **6c** and **6e** revealed, however, the presence of a second isomeric species, formed in essentially equal amount based on the peak intensities, a feature further discussed below. For **6a**, **6b** and **6d** the ^1H and $^{11}B-\{^1H\}$ NMR spectra establish the presence of the exopolyhedral B–H⟶Pt bond. Thus the ^1H NMR spectrum of **6b** shows a broad doublet signal at δ −8.59 [*J*(PH) 82 Hz] with ^{195}Pt satellite peaks [*J*(PtH) 445 Hz], and the $^{11}B-\{^1H\}$ spectrum displays a relatively deshielded and broad resonance for one boron nucleus at δ 27.3, the remaining signals being very broad and unresolved (Table 3). The ^1H and ^{11}B chemical shifts for the B–H⟶Pt group of **6b** agree well with those recorded previously for many other compounds containing B–H⟶M bonds.[2a,5] The $^1H-^{11}B$ coupling in either the ^1H or ^{11}B NMR spectra is evidently unresolved by the broadness of the peaks.

The $^{13}C-\{^1H\}$ NMR spectra (Table 2) of complexes **6a**, **6b** and **6d** all show resonances due to the presence of CO ligands. For **6d** two signals are seen for the three carbonyl ligands at δ 235.5 and 232.6, with relative intensity 1:2. Both resonances are doublets [*J*(PC) 5 Hz], and interestingly the signal at δ 232.6 displays weak $^{195}Pt-^{13}C$ coupling (49 Hz) in agreement with the earlier suggestion that CO groups may semi-bridge the Group 6 metal–platinum bonds in these species. The $^{13}C-\{^1H\}$ NMR spectrum of **6b** is less well resolved showing a multiplet for the three CO groups, while that for **6a** is a broad singlet, probably due to traces of paramagnetic impurity. An important feature of the $^{13}C-\{^1H\}$ NMR spectra of the three compounds is the observation of only two signals for the cage CMe groups, *e.g.* at δ 65.6 (*C*Me) and 31.1 (C*Me*) for **6b**. The equivalence of the two CMe moieties in these species indicates that the B–H⟶Pt three-centre two-electron bridge bonds must involve the boron atom β to the two carbons in the open CCB*B*B ring ligating the Group 6 metal. The two CMe fragments would be equivalent only with this arrangement, due to the presence of a symmetry plane through the metal atom, the β-B atom, and the midpoint of the cage C–C connectivity. It may be noted that it is generally the β-BH vertex of the open C_2B_3 ring which is activated when the $\eta^5-C_2B_9H_9Me_2$ ligand adopts a non-spectator role in forming an exopolyhedral B–H⟶M linkage.[1]

The $^{31}P-\{^1H\}$ NMR spectra (Table 3) of complexes **6a**, **6b** and **6d** are as expected, the non-equivalent PR_3 groups giving rise to two doublet signals with strong $^{195}Pt-^{31}P$ coupling. The resonance associated with the smaller *J*(PtP) value (*ca.* 2400–2600 Hz) is broader and is assigned to the PR_3 ligand transoid to the B–H⟶Pt bond. As expected, the ^{31}P resonance with the larger *J*(PtP) value (*ca.* 3700–4100 Hz) must then be attributed to the phosphine group transoid to the metal–metal bond.

As mentioned above, complexes **6c** and **6e** were each formed as a mixture of two isomers, present in approximately equal amounts. Although most clearly evident from the NMR data, discussed below, the existence of a second species was indicated from the IR spectra. Both **6c** and **6e** showed five CO stretching bands, rather than the three of **6a**, **6b** and **6d**. An explanation for the occurrence of isomers of **6c** and **6e** is found in earlier work.[2a] Compounds **1c** and **1d** were isolated as an inseparable mixture, and this mixture on treatment with CO afforded three products also inseparable. Nevertheless, X-ray diffraction studies firmly identified two of the compounds as **2c** and **6e**, with the third almost certainly being **2d**, an isomer of **6e** with a bridging hydrido ligand and a B–Pt σ bond. Moreover, spectroscopic

Table 1 Analytical[a] and physical data for the complexes

Compound	Colour	Yield (%)	$\nu_{max}(CO)$[b]/cm^{-1}	Analysis (%) C	Analysis (%) H
6a $[CrPt(CO)_3(PPh_3)_2(\eta^5\text{-}C_2B_9H_9Me_2)]$[c]	Red	31	1946s, 1887m, 1869m		
6b $[MoPt(CO)_3(PPh_3)_2(\eta^5\text{-}C_2B_9H_9Me_2)]$	Red	29	1963s, 1885m, 1869m	48.4 (48.7)	4.5 (4.3)
6c $[WPt(CO)_3(PPh_3)_2(\eta^5\text{-}C_2B_9H_9Me_2)]$[d]	Red	34	*2015s, 1959s, *1908m, 1877m, 1858m	45.0 (45.0)	4.1 (4.0)
6d $[MoPt(CO)_3(PEt_3)_2(\eta^5\text{-}C_2B_9H_9Me_2)]$	Orange	44	1954s, 1876m, 1857m	29.9 (29.6)	6.3 (5.9)
6e $[WPt(CO)_3(PEt_3)_2(\eta^5\text{-}C_2B_9H_9Me_2)]$[d]	Orange	37	*2014s, 1951s, *1901s, 1866m, 1850m	27.1 (26.5)	5.3 (5.3)
7a $[MoPt(CO)_3(PPh_3)_2(\eta^6\text{-}C_2B_{10}H_{10}Me_2)]$	Orange	35	1989vs, 1929m, 1888s	48.0 (48.2)	4.3 (4.3)
7b $[WPt(CO)_3(PPh_3)_2(\eta^6\text{-}C_2B_{10}H_{10}Me_2)]$	Orange	31	1984vs, 1923m, 1883s	44.7 (44.5)	4.3 (4.0)
7c $[MoPt(CO)_3(PEt_3)_2(\eta^6\text{-}C_2B_{10}H_{10}Me_2)]$	Orange	36	1983vs, 1916m, 1878s	28.8 (29.1)	6.1 (5.9)
7d $[WPt(CO)_3(PEt_3)_2(\eta^6\text{-}C_2B_{10}H_{10}Me_2)]$	Orange	37	1978vs, 1910m, 1873s	26.1 (26.2)	5.5 (5.3)
7e $[MoPt(CO)_4(PPh_3)(\eta^6\text{-}C_2B_{10}H_{10}Me_2)]$	Red	59	2087s, 2012vs, 1960m, 1924s	[e]35.4 (36.2)	4.4 (3.7)
7f $[WPt(CO)_4(PPh_3)(\eta^6\text{-}C_2B_{10}H_{10}Me_2)]$	Red	82	2086s, 2007vs, 1951m, 1917s	34.4 (33.7)	4.0 (3.4)
8a $[PtH(PPh_3)_3][MoPt(\mu\text{-}\sigma:\eta^6\text{-}C_2B_{10}H_9Me_2)(CO)_4(PPh_3)]$	Yellow	65	2017s, 1946vs, 1879m, 1855s	52.0 (52.8)	4.9 (4.2)
8b $[PtH(PPh_3)_3][WPt(\mu\text{-}\sigma:\eta^6\text{-}C_2B_{10}H_9Me_2)(CO)_4(PPh_3)]$	Yellow	34	2018s, 1942vs, 1874m, 1848s	50.2 (50.4)	4.7 (4.0)

[a] Calculated values are given in parentheses. [b] Measured in CH_2Cl_2. All spectra show a broad band at *ca.* 2550 cm^{-1} due to B–H absorptions. [c] Complex unstable, microanalytical data unsatisfactory, see text. [d] Infrared and NMR studies reveal two isomers present (*ca.* 1:1 ratio). The IR bands asterisked are assigned to the isomer with W(μ-H)Pt and B–Pt groups, see text. For complexes **6b**, **6d**, **7b**–**7d** traces of a second isomer were detected. [e] Crystallised with 0.5 molecule of CH_2Cl_2.

measurements on partially separated mixtures[2a] indicated an equilibrium between **2d** and **6e**. Evidently the reaction between the reagents $Tl[TlC_2B_9H_9Me_2]$, $[W(CO)_3(NCMe)_3]$ and $[PtCl_2(PR_3)_2]$, reported in this paper, also affords a mixture of the two isomers **2d** and **6e**.

In the earlier work[2a] the molecules **2c**, **2d** and **6e** cocrystallised, and the X-ray study revealed an asymmetric unit containing two crystallographically and chemically distinct molecules, one of which was **6e**. However, the other exhibited disorder as a result of a partial occupancy (1:4) of H and Et groups at one crystallographic site due to the presence of both **2c** and **2d**. For **2c** the X-ray data unambiguously established that the B–Pt bond involves a boron α to the cage CMe vertices. However, due to the 20% site occupancy, the species **2d** makes a relatively small contribution to the observed structure factors, and therefore platinum bonding to the β-boron in the CCB*B*B ring was not completely ruled out for this molecule.

In an attempt to resolve unequivocally whether in complex **2d** the B–Pt σ bond involves a boron atom α or β to the cage carbons in the C_2B_3 ring, crystals for an X-ray diffraction study were grown from solutions having a *ca.* 50% mixture of **6e** and **2d**. It was hoped that the crystals would contain both molecules as previously found, but without the complication of **2c**, the third component of the earlier mixture also being present in the solid state. The new study revealed, however, that only molecules of isomer **6e** were present in the crystal. The structural parameters were within experimental error the same as those obtained earlier,[2a] and are therefore not repeated herein. Nevertheless, this result provides a firm structural assignment for all the complexes **6** reported in this paper, and in particular establishes the presence in these molecules of the B_β–H→Pt bond.

The interconversion of the two isomers **6e** and **2d**[2a] requires the making and breaking of B_β–H→Pt and B_α–Pt linkages and the concomitant formation of B_α–H→Pt and B_β–Pt bonds, a process necessitating rotation of the *nido* face of the C_2B_9 cage at some stage. There is a precedent for the latter step. As previously mentioned, compound **3** releases hydrogen to yield **4**, but formation of the latter is accompanied by a small amount of an isomer with a B_α–Pt linkage. To account for this, rotation of the C_2B_3 ring ligating the metal atom in **3** was invoked.[2c]

The NMR data are in complete accord with the equilibrium between isomers shown in Scheme 1. The ^{11}B-{^{1}H} NMR spectrum of the mixture of complexes **6e** and **2d** (Table 3), shows two deshielded peaks at δ 23.5 and 44.0, each corresponding in intensity to one boron nucleus. The former resonance may be assigned to the B–H→Pt bridge system in **6e** and the latter, a doublet with ^{195}Pt satellite peaks [*J*(PB) 74, *J*(PtB) *ca.* 600 Hz], to the B–Pt group in **2d**. The two very broad resonances in the ^{31}P-{^{1}H} NMR spectrum at δ 9.6 and 16.0 are due to the isomer with the B–Pt bond, and the doublets at δ 15.1 and 21.4 can be attributed to molecules with the B–H→Pt linkage. The ^{31}P data are superior to those recorded earlier[2a] on a mixture which also contained **2c**, and lead to some reassignment of signals between the latter and **2d**.

The structure of complex **2d**,[2a] with a B_α–Pt bond, is supported by the observation from the ^{13}C-{^{1}H} NMR spectrum (Table 2) that the two cage CMe vertices are not equivalent, showing two resonances for the *C*Me nuclei (δ 64.1 and 62.9) and two for the C*Me* groups (δ 37.0 and 32.1). If **2d** had contained an exopolyhedral B_β–Pt bond then only one *C*Me and one C*Me* signal would be anticipated, assuming coplanarity of the μ-H, the two P, and the B_β atoms, resulting from the usual planar geometry around the platinum. This structure would result in the CMe groups being symmetrically disposed on either side of a plane of symmetry. As expected, the symmetrical isomer **6e**, with the B_β–H→Pt group, displays two CMe signals [δ 67.9 (*C*Me) and 32.7 (C*Me*)]. The ^{1}H NMR spectrum of the isomeric mixture was also informative, and like the ^{31}P-{^{1}H} NMR spectrum superior in quality to that measured previously when compound **2c** was also present.[2a] Two high-field resonances are seen (Table 2) at δ −9.14 [d of d, *J*(PH) 52 and 16, *J*(PtH) 377, and *J*(WH) 43 Hz] and at −7.07 (br s). These are diagnostic for the W(μ-H)Pt and the B–H→Pt groups in the respective isomers.

A similar analysis of the NMR data for complex **6c** establishes that in solution an isomer $[WPt(\mu\text{-}H)(\mu\text{-}\sigma:\eta^5\text{-}C_2B_9H_8Me_2)(CO)_3(PPh_3)_2]$ is present. The chromium–platinum compound **6a** showed no evidence for a second isomer, but the spectra of the Mo–Pt complexes **6b** and **6d** did reveal in their ^{1}H NMR spectra a very weak doublet-of-doublets signal attributable to isomers with Mo(μ-H)Pt bonds [**6b**, δ −7.90 with *J*(PH) 52 and 16, and *J*(PtP) *ca.* 400 Hz; **6d**, δ −8.22 with *J*(PH) 50 and

Table 2 Hydrogen-1 and carbon-13 NMR data[a] for the complexes

Compound	^{1}H[b] (δ)	^{13}C[c] (δ)
6a	−6.59 [br s, 1 H, BHPt, *J*(PtH) 497], 1.82 (s, 6 H, Me), 7.01–7.42 (m, 30 H, Ph)	242.2 (br s, 3 × CO), 137.7–128.5 (Ph), 67.3 (br s, *C*Me), 30.4 (C*Me*)
6b	−8.59 [br d, 1 H, BHPt, *J*(PH) 82, *J*(PtH) 445], 1.90 (s, 6 H, Me), 6.95–7.34 (m, 30 H, Ph)	234.4 (m, 3 × CO), 134.9–127.9 (Ph), 65.6 (*C*Me), 31.1 (C*Me*)
6c[d]	−8.42* [d of d, 1 H, μ-H, *J*(PH) 59, 16, *J*(PtH) 438, *J*(WH) 41], −6.10 (br s, 1 H, BHPt), 2.09 (s, 6 H, Me), 2.13*, 2.26* (s × 2, 6 H, Me), 6.93–7.39 (m, 30 H, Ph)	230.5 [d, CO, *J*(PC) 4], 225.0 [d of d, 2 × CO, *J*(PC) 7, 2], 219.0* (2 × CO), 216.6* (CO), 135.1–127.7 (Ph), 68.7 (*C*Me), 63.0* (*C*Me), 62.8* [t, *C*Me, *J*(PC) 3], 37.3*, 32.5* (C*Me*), 32.3 (C*Me*)
6d	−7.62 (br s, 1 H, BHPt), 1.01–1.27 (m, 18 H, CH_2*Me*), 1.97 (s, 6 H, Me), 2.01–2.26 (m, 12 H, CH_2)	235.5 [d, CO, *J*(PC) 5], 232.6 [d, 2 × CO, *J*(PC) 5, *J*(PtC) 49], 65.3 (*C*Me), 31.1 (C*Me*), 20.5 [d, CH_2, *J*(PC) 30, *J*(PtC) 30], 20.0 [d, CH_2, *J*(PC) 37, *J*(PtC) 44], 9.2 [d, CH_2*Me*, *J*(PC) 3, *J*(PtC) 28], 8.2 [d, CH_2*Me*, *J*(PC) 3, *J*(PtC) 19]
6e[d]	−9.14* [d of d, 1 H, μ-H, *J*(PH) 52, 16, *J*(PtH) 377, *J*(WH) 43], −7.07 (br s, 1 H, BHPt), 0.98–1.25 (m, 18 H, CH_2*Me*), 1.96–2.32 (m × 2, 18 H, CH_2 and Me)	225.0, 223.0* (CO), 220.8 (2 × CO), 215.5* [2 × CO, *J*(PtC) 46], 67.9 (*C*Me), 64.1* [*C*Me, *J*(PtC) 37], 62.9* (*C*Me), 37.0* [C*Me*, *J*(PtC) 35], 32.7 (C*Me*), 32.1* (C*Me*), 20.6–19.6, 17.9–17.0 (m × 2, CH_2), 9.4–8.0 (m, CH_2*Me*)
7a	[e] −4.78 [br d, 1 H, BHPt, *J*(PH) 83, *J*(PtH) 477], 1.46, 2.48 (s × 2, br, 6 H, CMe), 6.47–8.20 (m, 30 H, Ph)	[f] 222.6 (m, CO), 221.5 (m, 2 × CO), 135.5–128.1 (Ph), 93.2, 71.1 (*C*Me), 34.1, 33.3 (C*Me*)
7b[g]	−4.39 [br d, 1 H, BHPt, *J*(PH) 75, *J*(PtH) 469], 1.59, 2.68 (s × 2, 6 H, CMe), 7.02–7.74 (m, 30 H, Ph)	213.7 (CO) 213.3[d, CO, *J*(PC) 5], 211.4 (CO), 137.6–126.7 (Ph), 86.7, 66.4 (*C*Me), 34.8, 33.8 (C*Me*)
7c[h]	−5.85 [br s, 1 H, BHPt, *J*(PtH) 451], 1.11–1.26 (m, 18 H, CH_2*Me*), 1.57 (br s, 3 H, CMe), 2.12–2.17 (m, 12 H, CH_2), 2.45 (br s, 3 H, CMe)	223.5 (m, CO), 221.8 [d, CO, *J*(PC) 5], 219.8 (br m, CO), 91.9, 71.5 (*C*Me), 34.0 (br, C*Me*), 20.5 [d, CH_2, *J*(PC) 31, *J*(PtC) 31], 19.6 [d of d, CH_2, *J*(PC) 3 and 38, *J*(PtC) 44], 9.3 [d, CH_2*Me*, *J*(PC) 4, *J*(PtC) 28], 8.6 [d, CH_2*Me*, *J*(PC) 4, *J*(PtC) 20]
7d[i]	−5.43 [br t, 1 H, BHPt, *J*(PH) 66, *J*(PtH) 443], 1.05–1.17 (m, 18 H, CH_2*Me*), 1.67 (br s, 3 H, CMe), 2.09–2.24 (m, 12 H, CH_2), 2.65 (br s, 3 H, CMe)	214.4 (br m, CO), 213.6 [d, CO, *J*(PC) 5], 209.4 (br m, CO), 85.3, 67.1 (*C*Me), 34.8, 34.1 (C*Me*), 20.4 [d, CH_2, *J*(PC) 29, *J*(PtC) 29], 19.7 [d of d, CH_2, *J*(PC) 4 and 36, *J*(PtC) 46], 9.3 [d, CH_2*Me*, *J*(PC) 2, *J*(PtC) 28], 8.5 [d, CH_2*Me*, *J*(PC) 2, *J*(PtC) 19]
7e[g]	−4.27 [br s, 1 H, BHPt, *J*(PtH) 615], 1.60, 2.57 (s × 2, 6 H, CMe), 7.36–7.58 (m, 15 H, Ph)	219.2 (br m, CO), 219.0 [d, CO, *J*(PC) 5], 216.2 (br m, CO), 187.8 [d, PtCO, *J*(PC) 9], 133.8–128.7 (Ph), 95.1, 75.0 (*C*Me), 34.6, 33.8 (C*Me*)
7f[g]	−3.80 [br s, 1 H, BHPt, *J*(PtH) 602], 1.69, 2.78 (s × 2, 6 H, CMe), 7.34–7.58 (m, 15 H, Ph)	209.6 [d, CO, *J*(PC) 5], 209.2 [d, CO, *J*(PC) 5], 204.6 [d, CO, *J*(PC) 8], 184.5 [d, PtCO, *J*(PC) 11], 133.6–128.8 (Ph), 88.5, 69.7 (*C*Me), 35.2, 34.1 (C*Me*)
8a[j]	−5.70 [AB_2MX, 1 H, PtH, *J*(*trans*-PH) 165, *J*(*cis*-PH) 12, *J*(PtH) 774], 1.58, 2.19 (s × 2, 6 H, CMe), 7.07–7.58 (m, 60 H, Ph)	225.0, 221.9, 220.1 (MoCO), 203.9 (PtCO), 133.4–127.4 (Ph), 77.0, 68.0 (*C*Me), 35.1, 33.4 (C*Me*)
8b[i]	−5.74 [AB_2MX, 1 H, PtH, *J*(*trans*-PH) 165, *J*(*cis*-PH) 12, *J*(PtH) 774], 1.71, 2.37 (s × 2, 6 H, CMe), 7.01–7.56 (m, 60 H, Ph)	218.1, 212.0, 210.7 (WCO), 203.9 (PtCO), 134.4–127.5 (Ph), 71.9, 63.3 (*C*Me), 35.7, 33.7 (C*Me*)

[a] Chemical shifts δ in ppm, coupling constants in Hz, measurements in CD_2Cl_2 at ambient temperatures unless otherwise stated. [b] Signals due to BH groups appear as broad unresolved resonances in the range δ *ca.* −2 to +3. [c] Hydrogen-1 decoupled, chemical shifts are positive to high frequency of $SiMe_4$ (δ 0.0). [d] Peaks asterisked are due to second isomer, see text. [e] Measured at 200 K. [f] Measured at 230 K. [g] Measured at 240 K. [h] Measured at 250 K. [i] Measured at 260 K. [j] Measured at 210 K.

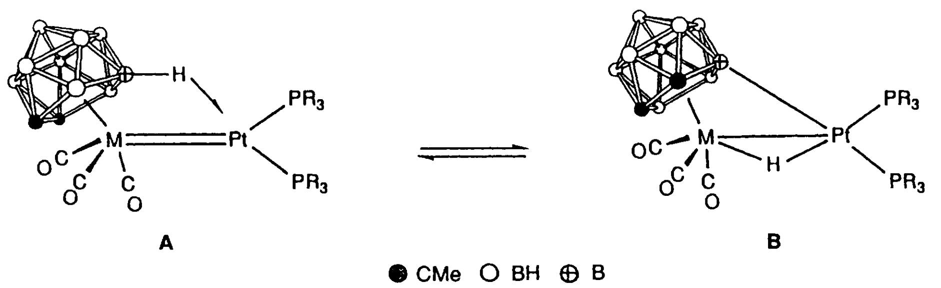

Scheme 1 M = Mo or W

17, and *J*(PtP) 380 Hz]. Structure **A** in Scheme 1 may be viewed as incipient oxidative addition of a B–H bond at the platinum centre, while **B** corresponds to completion of this process. Evidently **A** is the favoured species for most of these complexes, with the equilibrium between the isomers shifting towards **B** in the order Cr < Mo < W.

Reactions between the complexes $[PtCl_2(PR_3)_2]$ and the salts $Na_2[M(CO)_3(\eta^6\text{-}C_2B_{10}H_{10}Me_2)]$ (M = Mo or W) were next investigated. The sodium salts were generated *in situ* by reducing $C_2B_{10}H_{10}Me_2$ in thf with sodium dihydronaphthylide to obtain $Na_2[C_2B_{10}H_{10}Me_2]$[6] which was then treated with $[M(CO)_3(NCMe)_3]$. Addition of the platinum reagents to the mixture containing the species $Na_2[M(CO)_3(\eta^6\text{-}C_2B_{10}H_{10}Me_2)]$ afforded the dimetal compounds $[MPt(CO)_3(PR_3)_2(\eta^6\text{-}C_2B_{10}H_{10}Me_2)]$ **7a**–**7d**, characterised by the data given in Tables 1–3. These products, like the related compounds **6b**–**6e**, are stable in air over long periods and their solutions are also stable.

The NMR spectra were in accord with the formulations proposed, although it was observed that the molecules underwent dynamic behaviour, which is common in metal complexes containing the $\eta^6\text{-}C_2B_{10}H_{10}Me_2$ ligand.[7] Fluxionality of the C_2B_{10} cage causes equivalence of the CMe resonances in the ^{1}H NMR spectra of the compounds when measured at room temperature. For the molybdenum complexes **7a** and **7c** the CMe signals are broad, while for the tungsten species **7b** the

Table 3 Boron-11 and phosphorus-31 NMR data[a] for the complexes

Compound	^{11}B[b] (δ)	^{31}P[c] (δ)
6a	24.7 (1 B, BHPt), −6.5 to −9.9 (8 B)	29.2 [d, *J*(PP) 26, *J*(PtP) 2633], 27.2 [d, *J*(PP) 26, *J*(PtP) 4116]
6b	27.3 (1 B, BHPt), −9.2 to −12.0 (8B)	23.5 [d, *J*(PP) 19, *J*(PtP) 2565], 22.5 [d, *J*(PP) 19, *J*(PtP) 4125]
6c[d]	43.3* (BPt), 25.9 (BHPt), 2.4 to −9.1 (BH)	27.2* [vbr, *J*(PtP) *ca.* 1800], 24.9 [d, *J*(PP) 17, *J*(PtP) 4396], 21.0* [br, *J*(PtP) *ca.* 4200], 13.8 [d, *J*(PP) 17, *J*(PtP) 2489]
6d	24.2 (1 B, BHPt), −9.0 to −13.0 (8 B)	24.7 [d, *J*(PP) 19, *J*(PtP) 2437], 12.7 [d, *J*(PP) 19, *J*(PtP) 3746]
6e[d]	44.0* [br d, BPt, *J*(PB) 74, *J*(PtB) *ca.* 600], 23.5 (BHPt), 3.0 to −14.1 (BH)	21.4 [d, *J*(PP) 19, *J*(PtP) 4120], 16.0* (vbr, PEt$_3$), 15.1 [d, *J*(PP) 19, *J*(PtP) 2342], 9.6* [vbr, *J*(PtP) *ca.* 3800]
7a	24.9 (1 B, BHPt), −2.5 to −12.9 (9 B)	28.3 [d, *J*(PP) 22, *J*(PtP) 2600], 25.5 [br, *J*(PtP) 4117]
7b	21.3 [d, 1 B, BHPt, *J*(BH) 43], −2.0 to −9.5 (8 B), −14.8 (1 B)	22.3 [br, *J*(PtP) 4198], 17.7 [d, *J*(PP) 21, *J*(PtP) 2534]
7c	23.2 [d, 1 B, BHPt, *J*(BH) 67, *J*(PtB) 281], −0.5 to −6.0 (8 B), −13.7 (1 B)	26.1 [d, *J*(PP) 20, *J*(PtP) 2476], 11.9 [d, *J*(PP) 20, *J*(PtP) 3767]
7d	20.4 [d, 1 B, BHPt, *J*(BH) 67, *J*(PtB) 196], −2.7 to −6.8 (8 B), −15.1 (1 B)	16.7 [d, *J*(PP) 20, *J*(PtP) 2426], 9.9 [d, *J*(PP) 20, *J*(PtP) 3838]
7e	29.1 [1 B, BHPt, *J*(PtB) 287], −1.2 to −4.9 (8 B), −12.3 (1 B)	35.7 [s, *J*(PtP) 2579]
7f	24.6 [1 B, BHPt, *J*(PtB) 269], 0.5 to −5.6 (8 B), −13.7 (1 B)	27.3 [s, *J*(PtP) 2565]
8a	62.2 [1 B, *J*(PtB) 513], 0.7 to −8.0 (8 B), −16.3 (1 B)	35.6 [s, 1 P, *J*(PtP) 4286], 23.8 [m, 1 P, *trans*-P, *J*(PP) 19, *J*(PtP) 2235], 23.5 [m, 2 P, *cis*-P, *J*(PP) 19, *J*(PtP) 2820]
8b	58.5 [1 B, *J*(PtB) 525], −2.3 to −8.6 (8 B), −17.9 (1 B)	32.4 [s, 1 P, *J*(PtP) 4158], 23.6 [m, 1 P, *trans*-P, *J*(PP) 19, *J*(PtP) 2268], 23.5 [m, 2 P, *cis*-P, *J*(PP) 19, *J*(PtP) 2823]

[a] Chemical shifts δ in ppm, coupling constants in Hz, measurements in CD_2Cl_2 at ambient temperatures. [b] Hydrogen-1 decoupled, chemical shifts are positive to high frequency of $BF_3{\cdot}Et_2O$ (external). The ^{1}H–^{11}B couplings were measured from fully coupled ^{11}B NMR spectra. [c] Hydrogen-1 decoupled, chemical shifts are positive to high frequency of 85% H_3PO_4 (external). [d] Peaks asterisked are due to an isomer with a B–Pt bond, see text.

peak is very broad, and for **7d** too broad to be assigned a reasonably precise δ value. In the ^{13}C-{^{1}H} NMR spectra measured at room temperature the C*Me* groups also give rise to one resonance, and peaks for the cage-carbon nuclei were not seen. However, when the ^{1}H and ^{13}C-{^{1}H} NMR spectra are recorded at low temperatures (Table 2), the data clearly reveal non-equivalent CMe groups in the species **7a**–**7d**. Thus two CMe resonances are observed at δ 1.59 and 2.68 in the ^{1}H NMR spectrum of **7b**, when measured at 240 K, and correspondingly in the ^{13}C-{^{1}H} NMR spectrum, peaks are seen for non-equivalent CMe groups at δ 86.7 and 66.4 (*C*Me) and at δ 34.8 and 33.8 (C*Me*). In the spectrum of **7c** there is one broad C*Me* resonance, however two *C*Me signals are seen at δ 91.9 and 71.5. Compounds **7a**–**7d** all show in their IR spectra three carbonyl stretching bands, one of which occurs at a relatively low frequency (*ca.* 1880 cm^{-1}), suggesting that one CO group semi-bridges the metal–metal bond. In support of this proposal, it is noteworthy that in the ^{13}C-{^{1}H} NMR spectra of **7b**–**7d** one of the three CO resonances shows weak ^{31}P–^{13}C coupling (5 Hz).

It was of interest to determine if any of the compounds **7a**–**7d** existed in equilibrium with isomers [MPt(μ-H)(μ-σ:η^6-$C_2B_{10}H_9Me_2$)(CO)$_3$(PR$_3$)$_2$], structurally akin to **B** of Scheme 1. For **7a** no evidence for isomerism was obtained, but for **7b** and **7c** the ^{1}H NMR spectra showed diagnostic doublet of doublet resonances for a μ-H ligand at δ −7.99 [*J*(PH) 17 and 48] and −7.03 [*J*(PH) 18 and 39 Hz], respectively. Relative peak intensities revealed, however, that the isomers responsible for these signals were present only in trace amounts. The spectrum of **7d** also displayed a signal for a μ-H ligand [δ −8.48, d of d, *J*(PH) 17 and 42, *J*(PtH) 306 Hz], with the intensities of the peaks suggesting *ca.* 2% of this isomer to be present in the solutions. Remeasurement of the ^{1}H NMR spectrum of the same sample after 1 week showed no change, nor did recovery of the complex and recrystallisation affect the spectrum observed. This suggests an equilibrium between the two isomers very largely favouring the molecular structure of **7d** depicted.

The ^{31}P-{^{1}H} NMR spectra of compounds **7a**–**7d** were as expected (Table 3), each showing two resonances, with ^{195}Pt satellite peaks, for the non-equivalent PR$_3$ ligands. For **7c** and **7d** both resonances were doublets [*J*(PP) 20 Hz], but for **7a** and **7b** one of the resonances in each spectrum was a broad peak, and we assign these signals to the ^{31}PR$_3$ group transoid to the B–H→Pt bond, the broadening being the result of unresolved ^{31}P–^{11}B coupling. These broad resonances also had the larger ^{195}Pt coupling, as did the signals in the spectra of **7c** and **7d** at δ 11.9 and 9.9, respectively, which were also slightly broadened.

The ^{11}B-{^{1}H} and ^{1}H NMR spectra of the compounds **7a**–**7d** confirmed the existence of the exopolyhedral B–H→Pt bridge bonds. In each ^{11}B-{^{1}H} NMR spectrum there was one relatively deshielded resonance, with an intensity corresponding to one boron nucleus, and these were in the range δ 20.4–24.9. In the fully ^{1}H coupled spectra of **7b**–**7d** these resonances became doublets, and thus allowed measurement of ^{1}H–^{11}B couplings of *ca.* 43–67 Hz, values which are typical for such systems.[2c,5] The spectra of **7c** and **7d** were of sufficient resolution to reveal ^{11}B–^{195}Pt coupling of 281 and 196 Hz, respectively. The ^{1}H NMR spectra also displayed diagnostic resonances for the B–H→Pt units in the range δ −4.39 to −5.43. With the exception of **7c**, these signals (Table 2) showed ^{31}P and ^{195}Pt coupling of the expected magnitude. For **7c** the resonance was broad, the ^{31}P–^{1}H coupling being unresolved.

Treatment of a thf solution of Na$_2$[M(CO)$_3$(η^6-$C_2B_{10}H_{10}Me_2$)] (M = Mo or W) at −60 °C with [PtCl$_2$(cod)] (cod = cycloocta-1,5-diene), followed by 2 equivalents of PPh$_3$, afforded the salts [PtH(PPh$_3$)$_3$][MPt(μ-σ:η^6-$C_2B_{10}H_9Me_2$)(CO)$_4$(PPh$_3$)] **8**, data for which are given in Tables 1–3. The presence of the cation [PtH(PPh$_3$)$_3$]$^+$ in these products was established from their ^{1}H NMR data. The resonances at δ *ca.* −5.7 display the diagnostic AB$_2$MX pattern[8] for cations of the type [PtH(PR)$_3$)$_3$]$^+$.

The presence of the four carbonyl ligands in the compounds **8** is revealed by the observation of four CO stretching bands in their IR spectra (Table 1) accompanied by four CO resonances in the ^{13}C-{^{1}H} NMR spectra (Table 2). A peak at δ 203.9 is assigned to the PtCO group on the basis of its invariance between **8a** and **8b**, and its chemical shift. The two cage CMe groups display four peaks, and are thus non-equivalent in the limiting low-temperature spectra of these complexes. In the ^{31}P-{^{1}H} NMR spectra both salts show three resonances. The sharp singlets at δ 35.6 (**8a**) and 32.4 (**8b**) may be assigned to the Pt(CO)(PPh$_3$) fragments. Moreover, the PPh$_3$ ligand must be cisoid to the B–Pt bond and transoid to the Mo or W atoms

Table 4 Selected internuclear distances (Å) and angles (°) for the complex $[MoPt(CO)_4(PPh_3)(\eta^6\text{-}C_2B_{10}H_{10}Me_2)]$ **7e**

Mo–Pt	2.814(1)	Mo–C(1)	2.277(6)	Mo–B(2)	2.462(9)	Mo–C(3)	2.502(8)
Mo–B(4)	2.373(8)	Mo–B(5)	2.362(7)	Mo–B(6)	2.435(6)	Mo–C(5)	1.981(5)
Mo–C(6)	1.990(8)	Mo–C(7)	2.014(7)	C(1)–B(2)	1.549(12)	C(1)–B(6)	1.511(12)
C(1)–B(7)	1.785(10)	C(1)–C(2)	1.500(9)	B(2)–C(3)	1.732(9)	B(2)–B(7)	2.039(11)
B(2)–B(8)	1.824(12)	C(3)–B(4)	1.665(11)	C(3)–B(8)	1.746(9)	C(3)–B(9)	1.714(10)
C(3)–C(4)	1.533(10)	B(4)–B(5)	1.771(11)	B(4)–B(9)	1.794(12)	B(4)–B(10)	1.777(10)
B(5)–B(6)	1.847(10)	B(5)–B(10)	1.693(11)	B(5)–B(11)	1.709(9)	B(5)–H(5b)	1.101
B(6)–B(7)	1.976(13)	B(6)–B(11)	1.806(11)	B(7)–B(8)	1.901(13)	B(7)–B(11)	1.876(13)
B(7)–B(12)	1.784(11)	B(8)–B(9)	1.718(11)	B(8)–B(12)	1.724(12)	B(9)–B(10)	1.702(14)
B(9)–B(12)	1.743(10)	B(10)–B(11)	1.747(10)	B(10)–B(12)	1.734(11)	B(11)–B(12)	1.729(13)
C(5)–O(5)	1.152(7)	C(6)–O(6)	1.165(10)	C(7)–O(7)	1.178(9)	Pt–C(8)	1.851(6)
Pt–B(5)	2.313(8)	Pt–H(5b)	1.50	Pt–P	2.305(2)	C(8)–O(8)	1.154(8)
P–C(11)	1.825(6)	P–C(21)	1.807(7)	P–C(31)	1.814(6)		
Pt–Mo–C(5)	81.0(2)	Pt–Mo–C(6)	73.3(2)	Pt–Mo–C(7)	144.0(2)	Mo–C(5)–O(5)	175.0(7)
Mo–C(6)–O(6)	177.9(6)	Mo–C(7)–O(7)	178.4(7)	Mo–Pt–P	168.0(1)	Mo–Pt–C(8)	93.5(2)
Mo–Pt–H(5b)	75.3(3)	P–Pt–C(8)	98.4(2)	P–Pt–B(5)	114.2(2)	P–Pt–H(5b)	92.8(3)
C(8)–Pt–B(5)	146.3(3)	C(8)–Pt–H(5b)	168.8(4)	Pt–H(5b)–B(5)	124.8(3)	Pt–C(8)–O(8)	177.9(7)
Pt–P–C(11)	114.2(2)	Pt–P–C(21)	113.8(2)	Pt–P–C(31)	111.3(2)	C(11)–P–C(21)	105.6(3)
C(11)–P–C(31)	104.8(3)	C(21)–P–C(31)	106.4(3)				

Phenyl rings

	Mean	Range	Mean	Range
C(11)–C(16)	1.38(2)	1.36–1.41	120.0(7)	119.1–121.0
C(21)–C(26)	1.40(1)	1.39–1.41	120.0(6)	119.3–121.2
C(31)–C(36)	1.37(1)	1.36–1.39	120.0(9)	119.0–121.6

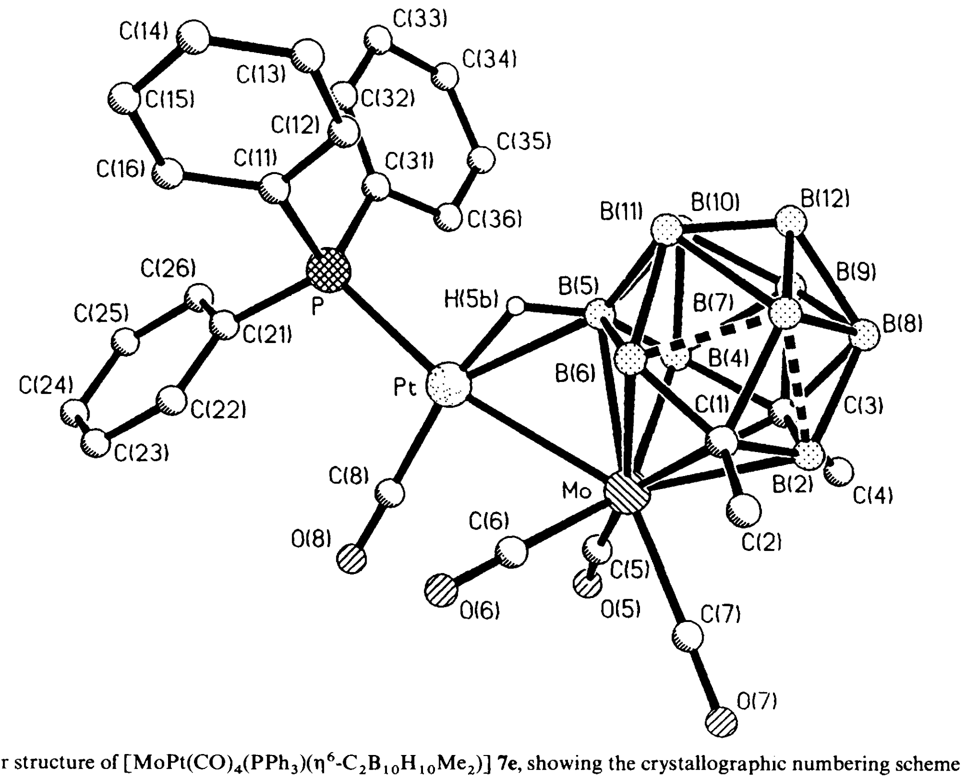

Fig. 1 The molecular structure of $[MoPt(CO)_4(PPh_3)(\eta^6\text{-}C_2B_{10}H_{10}Me_2)]$ **7e**, showing the crystallographic numbering scheme

because of the large $^{195}Pt\text{-}^{31}P$ couplings (*ca.* 4200 Hz). The presence of the B–Pt exopolyhedral bonds is clearly indicated by the $^{11}B\text{-}\{^1H\}$ NMR spectra. Each spectrum shows an appreciably deshielded resonance for one boron nucleus [δ 62.2 (**8a**) and 58.5 (**8b**)] with strong $^{195}Pt\text{-}^{11}B$ couplings of *ca.* 520 Hz. The pathway by which the compounds **8** form is unclear at the present time, but further studies are underway.

The nature of the salts **8** suggested that protonation might yield neutral complexes with the B–Pt bonds being replaced by B–H→Pt groups, and this was confirmed by experiment. Treatment of **8a** and **8b** with $HBF_4{\cdot}Et_2O$ in CH_2Cl_2 gave the complexes $[MPt(CO)_4(PPh_3)(\eta^6\text{-}C_2B_{10}H_{10}Me_2)]$ **7e** (M = Mo) and **7f** (M = W). It was also found that **7f** could be prepared by treating $[PtCl_2(CO)(PPh_3)]$ with $Na_2[W(CO)_3(\eta^6\text{-}C_2B_{10}H_{10}Me_2)]$. Moreover, treatment of **7e** with PPh_3 affords **7a** quantitatively. The structure of **7e** was established by X-ray diffraction analysis. Data from this study are summarised in Table 4 and the molecule is shown in Fig. 1.

The Mo–Pt bond [2.814(1) Å] is spanned by the *nido*-$C_2B_{10}H_{10}Me_2$ cage such that the latter is η^6-co-ordinated to the molybdenum and linked to the platinum *via* a three-centre two-electron bond B(5)–H→Pt. As expected, this bond involves the H atom attached to the boron atom which is β to the carbons in the CBCB*B*B face of the cage ligating the Mo atom. Although H(5b) was not directly located in the electron-density maps its position is in agreement with potential-energy minimisation calculations.[9] Moreover, its presence was unequivocally established by ^{1}H and ^{11}B-{^{1}H} NMR data discussed below. The Mo–Pt bond distance in **7e** is comparable with those found in the complexes [$Mo_2Pt_2(CO)_6(PPh_3)_2(\eta\text{-}C_5H_5)$] (average 2.838 Å)[10a] and [$MoPt_2(\mu_3\text{-}As)(CO)_4(PPh_3)_2(\eta\text{-}C_5H_5)$] (average 2.788 Å).[10b]

The non-planar character of the CBCBBB face of the carbaborane cage in complex **7e** is well evidenced by the appreciable variations in the distances of the six ring atoms from the molybdenum [Mo–C(1) 2.277(6), Mo–B(2) 2.462(9), Mo–C(3) 2.502(8), Mo–B(4) 2.373(8), Mo–B(5) 2.362(7), Mo–B(6) 2.435(6) Å]. The longest and shortest connectivities are associated with the two carbon atoms C(1) and C(3), a feature found in several other structures in which an MC_2B_{10} (Mo or W) cage system is linked to a metal–ligand group *via* exopolyhedral bonds.[2d,5a,7,11] Moreover, as expected, C(1) associated with the shortest separation from the Mo atom is the cage vertex with the lowest connectivity in the framework. Additionally, the long connectivities (shown in Fig. 1 by dashed lines) B(2) ··· B(7) [2.039(11)] and B(6) ··· B(7) [1.976(13) Å] involve the high-co-ordinate B(7) vertex and result in two square faces about C(1). The low-co-ordinate C(1) displays relatively short distances to B(2) [1.549(12)] and B(6) [1.511(12) Å]. These parameters are no doubt influenced by slippage of the cage to accommodate Mo–B(5) and Pt–B(5) distances of 2.362(7) and 2.313(8) Å, respectively.

The molybdenum atom carries three carbonyl ligands, bound in an essentially linear manner [Mo–C–O average 177.1(6)°]. The platinum atom is ligated by a PPh_3 group and by a CO molecule [Pt–C(8)–O(8) 177.9(7)°], with the former transoid to the molybdenum atom [P–Pt–Mo 168.0(1)°] and the latter transoid to the B(5)H(5b) unit [C(8)–Pt–H(5b) 168.8(4), C(8)–Pt–B(5) 146.3(3)°]. As mentioned above, the ^{195}Pt–^{31}P couplings in the ^{31}P-{^{1}H} NMR spectra of the salts **8** indicate that in these species also the PPh_3 ligands are transoid to the metal–metal bonds.

The complexes **7e** and **7f** are fluxional on the NMR time-scale. Thus in the ^{1}H NMR spectra, measured at room temperature, the cage CMe resonances appear as broad singlets, whereas at low temperatures (Table 2) two peaks are observed for **7e** at δ 1.60 and 2.57 and for **7f** at δ 1.69 and 2.78. Similarly, in the room-temperature ^{13}C-{^{1}H} NMR spectrum there is only one C*Me* resonance, and the *C*Me signals are not seen. However, in the limiting low-temperature spectra four CO resonances and four signals for the CMe groups are seen (Table 2). In the low-temperature ^{1}H NMR spectra of **7e** and **7f** there are broad singlet resonances for the B–H→Pt groups at δ −4.27 [*J*(PtH) 615 Hz] and −3.80 [*J*(PtH) 602 Hz], respectively. Correspondingly, in the ^{11}B-{^{1}H} NMR spectra there are resonances for the B–H→Pt system at δ 29.1 [*J*(PtB) 287] for **7e** and at 24.6 [*J*(PtB) 269 Hz] for **7f**. As expected, the ^{31}P-{^{1}H} NMR spectra show a single resonance for the Pt(CO)(PPh_3) groups.

The results described in this paper demonstrate that the anionic species [$M(CO)_3(\eta^5\text{-}C_2B_9H_9Me_2)$]$^{2-}$ and [$M(CO)_3(\eta^6\text{-}C_2B_{10}H_{10}Me_2)$]$^{2-}$ readily react with chloroplatinum complexes to yield compounds with bonds between platinum and molybdenum or tungsten. The carbaborane cage adopts a non-spectator role in the products, forming exopolyhedral B–H→Pt or B–Pt linkages. Studies are continuing with the dianionic molybdenum and tungsten reagents to synthesise other compounds having heteronuclear metal–metal bonds.

Experimental

Light petroleum refers to that fraction of b.p. 40–60 °C, and all solvents were freshly distilled over appropriate drying agents prior to use. Chromatography columns *ca.* 15 cm long and 3 cm in diameter were packed with alumina (Brockmann activity II) or silica (70–230 mesh). Celite pads were *ca.* 3 cm thick. All experiments were carried out under nitrogen using Schlenk-tube techniques. The NMR measurements were made using a Bruker AMX 360 MHz spectrometer and IR spectra were recorded with a Bruker IFS 25 instrument. The compounds [$M(CO)_3(NCMe)_3$][12] and the reagent Tl[$TlC_2B_9H_9Me_2$][4] were prepared as previously described. The salt $Na_2[C_2B_{10}H_{10}Me_2]$ was prepared *in situ*.

Table 5 Data for crystal structure analyses

Compound	**6e**	**7e**
Molecular formula	$C_{19}H_{45}B_9O_3P_2PtW$	$C_{26}H_{31}B_{10}MoO_4PPt\cdot 0.5CH_2Cl_2$
M	859.7	880.1
Crystal system	Monoclinic	Triclinic
Space group	$P2_1/n$ (no. 14)	$P\bar{1}$ (no. 2)
a/Å	8.0233(7)	9.2023(5)
b/Å	16.8325(7)	13.8017(6)
c/Å	23.2420(9)	15.1352(8)
α/°	90.0	109.376(4)
β/°	91.868(5)	91.059(4)
γ/°	90.0	101.054(4)
U/Å^3	3137.2(3)	1765.1(2)
Z	4	2
D_c/Mg m^{-3}	1.820	1.656
F(000)		850
μ(Mo-Kα)/cm^{-1}		44.97
T/K		292
Scan range, ω/°		1.20 + 0.34 tanθ
2θ Range/°		3.0–40.0
Radiation		Mo-Kα ($\bar{\lambda}$ = 0.710 73 Å)
Refined parameters		416
Data-to-parameter ratio		7.6:1
R,*R'* (R_{all})		0.030, 0.038 (0.031)

Preparation of the Complexes.—[$MPt(CO)_3L_2(\eta^5\text{-}C_2B_9H_9Me_2)$]. (*i*) A suspension of $Tl_2[Cr(CO)_3(\eta^5\text{-}C_2B_9H_9Me_2)]$ in thf (20 cm^3), prepared from [$Cr(CO)_3(NCMe)_3$] (0.1 g, 0.39 mmol) and Tl[$TlC_2B_9H_9Me_2$] (0.22 g, 0.39 mmol), was treated with [$PtCl_2(PPh_3)_2$] (0.31 g, 0.39 mmol), and stirred for 3 h, during which time a red colour developed and a precipitate, presumably TlCl, was formed. After this time the solution was filtered through a Celite pad, solvent was removed *in vacuo*, and the residue dissolved in CH_2Cl_2–light petroleum (4 cm^3, 1:1). The crude product was chromatographed on alumina using CH_2Cl_2–light petroleum (1:2) as the eluent. This procedure afforded a slow moving red band which was collected, and the solvent was removed *in vacuo*. Recrystallisation of the resultant oil from CH_2Cl_2–light petroleum (1:9) yielded red *microcrystals* of [$CrPt(CO)_3(PPh_3)_2(\eta^5\text{-}C_2B_9H_9Me_2)$] **6a** (0.15 g).

(*ii*) In a similar experiment a suspension of $Tl_2[Mo(CO)_3(\eta^5\text{-}C_2B_9H_9Me_2)]$ in thf (20 cm^3) was prepared from [$Mo(CO)_3(NCMe)_3$] (0.10 g, 0.33 mmol) and Tl[$TlC_2B_9H_9Me_2$] (0.19 g, 0.33 mmol), and treated with [$PtCl_2(PPh_3)_2$] (0.26 g, 0.33 mmol) to yield red *microcrystals* of [$MoPt(CO)_3(PPh_3)_2(\eta^5\text{-}C_2B_9H_9Me_2)$] **6b** (0.10 g).

(*iii*) Similarly, treatment of $Tl_2[W(CO)_3(\eta^5\text{-}C_2B_9H_9Me_2)]$, prepared from [$W(CO)_3(NCMe)_3$] (0.10 g, 0.26 mmol) and Tl[$TlC_2B_9H_9Me_2$] (0.15 g, 0.26 mmol), with [$PtCl_2(PPh_3)_2$] (0.21 g, 0.26 mmol) afforded red *microcrystals* of [$WPt(CO)_3(PPh_3)_2(\eta^5\text{-}C_2B_9H_9Me_2)$] **6c** (0.10 g).

(*iv*) Likewise, treatment of $Tl_2[Mo(CO)_3(\eta^5\text{-}C_2B_9H_9Me_2)]$, prepared from [$Mo(CO)_3(NCMe)_3$] (0.10 g, 0.33 mmol) and Tl[$TlC_2B_9H_9Me_2$] (0.19 g, 0.33 mmol), with [$PtCl_2(PEt_3)_2$] (0.17 g, 0.33 mmol) afforded orange *microcrystals* of [$MoPt(CO)_3(PEt_3)_2(\eta^5\text{-}C_2B_9H_9Me_2)$] **6d** (0.11 g).

Table 6 Atomic positional parameters (fractional coordinates, × 10^4) for compound **7e** with estimated standard deviations in parentheses

Atom	x	y	z	Atom	x	y	z
Mo	3 551(1)	7 135(1)	706(1)	O(8)	2 124(6)	3 972(4)	584(3)
C(1)	5 279(7)	8 663(5)	1 294(5)	P	1 519(2)	5 695(1)	3 231(1)
B(2)	4 185(8)	8 935(6)	667(6)	C(11)	2 781(6)	6 238(5)	4 303(4)
C(3)	2 275(7)	8 564(5)	657(4)	C(12)	3 333(7)	7 312(5)	4 649(5)
B(4)	1 551(8)	7 914(6)	1 351(5)	C(13)	4 213(7)	7 777(6)	5 481(5)
B(5)	2 860(7)	7 931(6)	2 231(5)	C(14)	4 525(7)	7 160(6)	5 987(5)
B(6)	4 858(8)	8 408(6)	2 165(5)	C(15)	3 987(7)	6 100(6)	5 660(5)
B(7)	4 669(8)	9 771(6)	2 065(6)	C(16)	3 098(7)	5 627(5)	4 797(4)
B(8)	3 086(8)	9 872(6)	1 298(6)	C(21)	1 048(6)	4 295(5)	2 994(4)
B(9)	1 459(8)	9 265(6)	1 600(6)	C(22)	2 121(7)	3 702(5)	2 651(5)
B(10)	1 801(8)	8 849(6)	2 509(6)	C(23)	1 766(7)	2 617(5)	2 433(5)
B(11)	3 686(8)	9 188(6)	2 904(6)	C(24)	362(8)	2 109(5)	2 538(5)
B(12)	2 908(8)	9 995(6)	2 460(5)	C(25)	−706(8)	2 695(6)	2 875(5)
C(2)	6 861(7)	8 803(6)	1 052(6)	C(26)	−362(7)	3 794(5)	3 100(4)
C(4)	1 427(8)	8 373(6)	−287(5)	C(31)	−158(6)	6 181(5)	3 568(4)
C(5)	1 973(7)	6 007(5)	−145(5)	C(32)	−517(6)	6 465(5)	4 487(4)
O(5)	1 059(6)	5 396(4)	−681(4)	C(33)	−1 787(7)	6 816(5)	4 727(5)
C(6)	5 004(7)	6 295(5)	867(4)	C(34)	−2 708(7)	6 890(6)	4 043(5)
O(6)	5 890(5)	5 828(4)	962(3)	C(35)	−2 350(7)	6 670(6)	3 142(5)
C(7)	4 400(7)	6 894(5)	−548(5)	C(36)	−1 082(7)	6 300(6)	2 894(5)
O(7)	4 899(7)	6 730(5)	−1 281(4)	C(99)	9 958(10)	915(7)	4 653(8)
Pt	2 437(1)	6 150(1)	1 983(1)	Cl(1)	10 720(7)	101(7)	5 156(5)
C(8)	2 225(7)	4 812(5)	1 111(5)	Cl(2)	8 307(7)	242(6)	3 916(5)

(*v*) In a similar manner, treatment of $Tl_2[W(CO)_3(\eta^5\text{-}C_2B_9H_9Me_2)]$, prepared from $[W(CO)_3(NCMe)_3]$ (0.10 g, 0.26 mmol) and $Tl[TlC_2B_9H_9Me_2]$ (0.15 g, 0.26 mmol), with $[PtCl_2(PEt_3)_2]$ (0.13 g, 0.26 mmol) afforded orange *microcrystals* of $[WPt(CO)_3(PEt_3)_2(\eta^5\text{-}C_2B_9H_9Me_2)]$ **6e** (0.08 g).

$[MPt(CO)_3L_2(\eta^6\text{-}C_2B_{10}H_{10}Me_2)]$. These compounds were prepared by similar procedures, which are described in detail for **7a** only. A solution of $C_2B_{10}H_{10}Me_2$ (0.07 g, 0.41 mmol) and naphthalene (*ca.* 0.02 g) in thf (10 cm^3) was stirred with sodium (*ca.* 0.1 g) until a green colour was formed, indicating that the carbaborane had been reduced to $Na_2[C_2B_{10}H_{10}Me_2]$. The latter was then added to $[Mo(CO)_3(NCMe)_3]$ (0.12 g, 0.40 mmol), with stirring for 20 min, to form *in situ* $Na_2[Mo(CO)_3(\eta^6\text{-}C_2B_{10}H_{10}Me_2)]$. The reagent $[PtCl_2(PPh_3)_2]$ (0.29 g, 0.37 mmol) was added, and the mixture stirred for 2.5 h. Solvent was then removed *in vacuo*, and the residue extracted with Et_2O–CH_2Cl_2 (3 × 10 cm^3, 2:1). The extracts were filtered through a Celite plug, and the solvent removed *in vacuo*. The residue was then dissolved in light petroleum–CH_2Cl_2 (*ca.* 3 cm^3, 3:2) and chromatographed on an alumina column. Eluting with the same solvent mixture afforded an orange fraction. After removing solvent from this eluate, the residue was crystallised from CH_2Cl_2–light petroleum to afford orange *microcrystals* of $[MoPt(CO)_3(PPh_3)_2(\eta^6\text{-}C_2B_{10}H_{10}Me_2)]$ **7a** (0.14 g). Further elution of the column with CH_2Cl_2 afforded a small amount of $[PtH(PPh_3)_3][MoPt(\mu\text{-}\sigma{:}\eta^6\text{-}C_2B_{10}H_9Me_2)(CO)_4(PPh_3)]$ **8a** (0.02 g).

$[PtH(PPh_3)_3][MPt(\mu\text{-}\sigma{:}\eta^6\text{-}C_2B_{10}H_9Me_2)(CO)_4(PPh_3)]$. A solution of $C_2B_{10}H_{10}Me_2$ (0.10 g, 0.59 mmol) in thf (10 cm^3) was reduced with an excess of sodium dihydronaphthylide and then added to $[Mo(CO)_3(NCMe)_3]$ (0.18 g, 0.61 mmol). After stirring for 10 min to generate $Na_2[Mo(CO)_3(\eta^6\text{-}C_2B_{10}H_{10}Me_2)]$ *in situ*, the solution was cooled to −60 °C and $[PtCl_2(cod)]$ (0.22 g, 0.59 mmol) was added. After stirring for 0.5 h the mixture was warmed to −40 °C and after 45 min PPh_3 (0.31 g, 1.18 mmol) was added. The mixture was then warmed to room temperature and stirred for 16 h. Solvent was removed *in vacuo*, and the residue extracted with CH_2Cl_2 (3 × 10 cm^3) and the extracts filtered through an alumina plug (5 × 2 cm). After removal of solvent *in vacuo*, the residue was dissolved in light petroleum–CH_2Cl_2 (*ca.* 5 cm^3, 1:1) and chromatographed on an alumina column. Eluting with the same solvent mixture afforded initially an orange fraction containing **7a** (0.01 g) and then on further elution with neat CH_2Cl_2 a yellow band. Removal of solvent *in vacuo* from the latter and precipitation from CH_2Cl_2–light petroleum afforded a yellow powder of $[PtH(PPh_3)_3][MoPt(\mu\text{-}\sigma{:}\eta^6\text{-}C_2B_{10}H_9Me_2)(CO)_4(PPh_3)]$ **8a** (0.35 g). Compound **8b** was prepared by a similar procedure.

$[MPt(CO)_4(PPh_3)(\eta^6\text{-}C_2B_{10}H_{10}Me_2)]$. Compounds **7e** and **7f** were prepared using a similar procedure which is described in detail for the former. To a solution of **8a** (0.06 g, 0.03 mmol) in CH_2Cl_2 (10 cm^3) was added one drop of $HBF_4{\cdot}Et_2O$. The mixture changed from yellow to red, and an IR spectrum showed complete consumption of the starting complex. Solvent was removed *in vacuo* and the residue was extracted with Et_2O–CH_2Cl_2 (3 × 10 cm^3, 2:1). The extracts were filtered through a Celite plug and the solvent was removed *in vacuo*. The residue was then dissolved in light petroleum–CH_2Cl_2 (*ca.* 5 cm^3, 2:1) and chromatographed on a silica column. Eluting with the same solvent mixture afforded **7e** as a red band, followed by a trace of orange **7a**. Removal of the solvent *in vacuo* afforded $[MoPt(CO)_4(PPh_3)(\eta^6\text{-}C_2B_{10}H_{10}Me_2)]$ **7e** as red *microcrystals* (0.02 g).

Crystal Structure Determinations.—Crystals of complexes **6e** and **7e** were grown by diffusion of light petroleum into CH_2Cl_2 solutions. Those of **7e** contained half a molecule of CH_2Cl_2 in the unit cell. A conoscopic examination of **7e**, using crystal rotation between two crossed polarizers on a Zeiss Photomicroscope (II), verified the optical quality and biaxial nature of the system. Data were obtained from a clear rectangular crystal (0.22 × 0.29 × 0.63 mm) on an Enraf-Nonius CAD4-F autodiffractometer equipped with a dense graphite monochromator (take-off angle 5.8°). As discussed earlier, an X-ray diffraction study was carried out on **6e**, but since the data obtained confirmed those previously reported[2a] they are not repeated here, except for those given in Table 5 which were not available from the earlier study on a crystal also containing molecules **2c** and **2d**. Also listed in Table 5 are the crystal data for **7e** and other pertinent experimental details for this complex. The final unit-cell constants for **7e** were determined at high angles ($30.0 < 2\theta < 40.0°$). The ω–2θ scan technique was employed with a variable scan rate of 0.46–3.44° min^{-1} in ω using molybdenum radiation (h 0 to 8, k −13 to 13, l −14 to 14). The intensities of the monitored standard reflections measured as a function of time (every 2 h) showed an overall decay of 7.9% (a rate of −0.0689% h^{-1}) which required a maximum correction of 1.041 87. An empirical high-angle ψ-scan absorption correction (maximum, minimum transmission factors = 1.0000, 0.8678) was applied after correction for Lorentz and polarisation effects. After averaging the independent data (3291, $R_{int} = 0.010$), 3172 were unique [$F \geqslant 4.0\sigma(F)$] and used in the structure analysis.

The phase problem was solved by direct and Fourier methods, and all non-hydrogen atoms were anisotropically refined using the conventional blocked-cascade least-squares method.[13] Hydrogen atoms were included at calculated positions (C–H 0.96, B–H 1.10 Å) with fixed isotropic thermal parameters (80 and 60 × 10^{-3} Å^2 respectively). The final cycle of refinement which included a secondary extinction correction [$g = 1.2(6) \times 10^{-4}$ e^{-2}] yielded reliability factors of $R = [\Sigma(||F_o| - |F_c||)/\Sigma|F_o|] = 0.030$ and $R' = [\Sigma w(|F_o| - |F_c|)^2/\Sigma w|F_o|^2]^{\frac{1}{2}} = 0.038$ and a 'goodness-of-fit' value of $S = 1.64$. The minimised quantity was $\Sigma w||F_o| - |F_c||^2$ and the weighting factor $w = [\sigma^2(F) + 0.0006F^2]^{-1}$. A final electron-density map displayed some residual density in the vicinity of the Pt atom which is considered quite normal when dealing with heavy metal atoms. However, elsewhere only a random fluctuating background was observed. Atomic scattering factors and associated anomalous dispersion correction factors were taken from the usual source.[14] Final fractional atomic coordinates for non-hydrogen atoms are listed in Table 6.

Additional material available from the Cambridge Crystallographic Data Centre comprises H-atom coordinates, thermal parameters, and remaining bond distances and angles for **7e**, and atomic coordinates, thermal parameters and bond distances and angles for compound **6e**.

Acknowledgements

We thank the Robert A. Welch Foundation for support (Grants AA-1201 and 0668), the University of Kent at Canterbury for study leave (to M. J. W.), and Dr. N. Carr for helpful discussions.

References

1 F. G. A. Stone, *Adv. Organomet. Chem.*, 1990, **31**, 53.

2 (*a*) M. J. Attfield, J. A. K. Howard, A. N. de M. Jelfs, C. M. Nunn and F. G. A. Stone, *J. Chem. Soc., Dalton Trans.*, 1987, 2219; (*b*) J. C. Jeffery, M. D. Mortimer and F. G. A. Stone, *Inorg. Chim. Acta*, 1992, **198**, 593; (*c*) D. D. Devore, J. A. K. Howard, J. C. Jeffery, M. U. Pilotti and F. G. A. Stone, *J. Chem. Soc., Dalton Trans.*, 1989, 303; (*d*) N. C. Carr, M. C. Gimeno and F. G. A. Stone, *J. Chem. Soc., Dalton Trans.*, 1990, 2617; (*e*) F.-E. Baumann, J. A. K. Howard, R. J. Musgrove, P. Sherwood and F. G. A. Stone, *J. Chem. Soc., Dalton Trans.*, 1988, 1879.

3 (*a*) M. F. Hawthorne, D. C. Young, T. D. Andrews, D. V. Howe, R. L. Pilling, A. D. Pitts, M. Reintjes, L. F. Warren and P. A. Wegner, *J. Am. Chem. Soc.*, 1968, **90**, 879; (*b*) Y. Do, C. B. Knobler and M. F. Hawthorne, *J. Am. Chem. Soc.*, 1987, **109**, 1853; (*c*) J. Kim, Y. Do, Y. S. Sohn, C. B. Knobler and M. F. Hawthorne, *J. Organomet. Chem.*, 1991, **418**, C1.

4 J. L. Spencer, M. Green and F. G. A. Stone, *J. Chem. Soc., Chem. Commun.*, 1972, 1178.

5 (*a*) S. A. Brew, N. Carr, M. D. Mortimer and F. G. A. Stone, *J. Chem. Soc., Dalton Trans.*, 1991, 811; (*b*) J. R. Fernandez, G. F. Helm, J. A. K. Howard, M. U. Pilotti and F. G. A. Stone, *J. Chem. Soc., Dalton Trans.*, 1990, 1747 and refs. therein.

6 D. F. Dustin, G. B. Dunks and M. F. Hawthorne, *J. Am. Chem. Soc.*, 1973, **95**, 1109.

7 S. J. Crennell, D. D. Devore, S. J. B. Henderson, J. A. K. Howard and F. G. A. Stone, *J. Chem. Soc., Dalton Trans.*, 1989, 1363.

8 T. W. Pringle and K. R. Dixon, *Inorg. Chem.*, 1974, **13**, 846; R. G. Goel and R. C. Srivastava, *J. Organomet. Chem.*, 1983, **244**, 303.

9 A. G. Orpen, *J. Chem. Soc., Dalton Trans.*, 1980, 2509.

10 (*a*) R. Bender, P. Braunstein, Y. Dusansoy and J. Protas, *J. Organomet. Chem.*, 1979, **172**, C51; (*b*) M. Gorzellik, B. Nuber, T. Bohn and M. L. Ziegler, *J. Organomet. Chem.*, 1992, **429**, 173.

11 N. Carr, J. R. Fernandez and F. G. A. Stone, *Organometallics*, 1991, **10**, 2718.

12 G. J. Kubas and L. S. van der Sluys, *Inorg. Synth.*, 1990, **28**, 29; D. P. Tate, W. R. Knipple and J. M. Augl, *Inorg. Chem.*, 1962, **1**, 433.

13 SHELXTL-PC, Siemens Analytical X-ray Instruments, Madison, WI, 1989.

14 *International Tables for X-Ray Crystallography*, Kynoch Press, Birmingham, 1974, vol. 4.

Received 10*th July* 1992; *Paper* 2/03655J